

Rapid Synthesis of SeO₂ Nanoparticles and Their Activity Against Clinical Isolates (Gram positive, Gram negative, and Fungi)

Mustafa Younis Ali¹, Wedian K. Abad², Harakat Mohsin Roomy³ and Ahmed N. Abd^{1*}

¹Physics Department, Faculty of Science, Mustansiriyah University, Baghdad, Iraq

²Applied Physics Branch, Department of Applied Science, University of Technology, Iraq

³Department of physics, Ministry of Education, Baghdad, Iraq

*Correspondence to:

Ahmed N. Abd

Physics Department, Faculty of Science,
Mustansiriyah University, Baghdad, Iraq.

E-mail: ahmednaji_abd@yahoo.com

Received: August 16, 2023

Accepted: August 30, 2023

Published: September 06, 2023

Citation: Ali MY, Abad WK, Roomy HM, Abd AN. 2023. Rapid Synthesis of SeO₂ Nanoparticles and Their Activity Against Clinical Isolates (Gram positive, Gram negative, and Fungi). *NanoWorld J* 9(3): 89-93.

Copyright: © 2023 Ali et al. This is an Open Access article distributed under the terms of the Creative Commons Attribution 4.0 International License (CCBY) (<http://creativecommons.org/licenses/by/4.0/>) which permits commercial use, including reproduction, adaptation, and distribution of the article provided the original author and source are credited.

Published by United Scientific Group

Abstract

This study outlines a prompt method for the production of selenium oxide nanoparticles (SeO₂-NPs) utilizing selenium disulfide (SeS₂) and ethanol. The SeO₂-NPs were subjected to characterization utilizing X-ray diffraction (XRD), atomic force microscopy (AFM), ultraviolet spectroscopy, and Fourier transform infrared (FT-IR) spectroscopy techniques. The results indicate the existence of SeO₂-NPs, which exhibit an average size of about < 20 nm. The XRD pattern obtained from the SeO₂-NPs indicates the presence of a hexagonal crystal lattice. The objective of this article was to investigate the characteristics of SeO₂-NPs that possess antibacterial and antifungal properties. The efficacy of NPs as an antibacterial and antifungal agent has been demonstrated through examinations conducted on *Staphylococcus aureus*, *Staphylococcus epidermidis*, *Klebsiella*, *Escherichia coli*, and *Candida*.

Keywords

Nanoparticles, Selenium oxide, Chemical method, Antimicrobial, Antifungal

Introduction

Antimicrobial agents have been employed for a considerable duration to prevent or eradicate bacteria and other microorganisms. Nonetheless, the efficacy of these medications has been significantly reduced over time due to microbial resistance, which remains a persistent concern [1]. The utilization of NPs represents a highly auspicious approach in the fight against microbial resistance. The emergence of multidrug-resistant organisms (MDROs) has posed a significant challenge in the management of healthcare-associated infections, rendering current medications less effective. The prevalence of infections caused by MDROs is on the rise, leading to increased rates of illness and death globally. The process of developing novel antibiotics is a resource-intensive endeavor, involving significant financial and labor investments. The treatment of MDRO infections involves the administration of high doses of antibiotics, which may result in adverse and undesirable effects. Therefore, alternative approaches need to be developed. The utilization of NPs is a prospective approach for the management of infections caused by MDROs. NPs have exhibited potential therapeutic benefits owing to their unique physical and chemical properties. NPs possess antimicrobial activity that can effectively counteract common resistance mechanisms exhibited by antimicrobial agents, including enzyme inactivation, reduced cell permeability, target site/enzyme modification, and enhanced efflux through overexpression of efflux pumps [2, 3]. NPs present themselves as a viable substitute for traditional antibiotics owing to their unique characteristics. The heightened surface-to-volume ratio of NPs results in an augmented interaction surface with target organ-

isms. NPs have the ability to act as molecular agents at the nanoscale level, thereby enabling them to interact with bacterial cells, regulate the permeability of cell membranes, and impede molecular pathways. Furthermore, it is possible that NPs could enhance the inhibitory effects of antibiotics. During the manufacturing process of NPs, various physicochemical features such as size, shape, chemical modification, solvent, and ambient conditions can impact the antibacterial properties of the NPs and their interaction with bacteria [4]. A newly identified category of potential anti-bacterial agents, known as selenium NPs (SeNPs), has been discovered. Selenium is a vital micronutrient in biological systems, possessing various properties such as anticancer and anti-bacterial effects, antioxidant capabilities, and modulation of the immune system. These attributes offer a diverse array of potential applications in the fields of biology and medicine, including the utilization of nutritional supplements. Notwithstanding their beneficial properties, toxic variations of selenium such as selenite (SeO₄⁻²), selenite (SeO₃⁻²), and selenide (Se⁻²) are present in the natural surroundings. The primary objective of the present study is to effectively exhibit the chemical synthesis of SeO₂-NPs and the efficacy of said NPs against bacterial and fungal organisms [5-8]. This research provides valuable insights into the potential applications of SeO₂-NPs in the medical domain, particularly in the context of antibacterial and antifungal therapeutics.

Experimentation

SeO₂-NPs may be synthesized via the utilization of SeS₂. SeS₂ was dissolved in 100 ml of ethanol, resulting in an orange-colored liquid solution with a mass of approximately 0.715 g. The experimental procedure involved placing the solution on a magnetic stirrer for a duration of one hour at a temperature of 50 °C. Subsequently, drops of sodium hydroxide were added with caution, leading to the formation of a brown nano-solution as depicted in figure 1, resulting from the reaction of SeS₂. In order to investigate the formation of SeO₂-NPs, the solution is applied onto a pristine glass substrate using the drop casting technique, with the aim of conducting XRD (XRD-6000, Shimadzu X-ray diffractometer) using CuKα X-ray source and AFM analyses (AA 3000 scanning probe microscope).

Results and Discussion

XRD was used to determine the crystalline structure of the SeO₂-NPs. The characteristic peaks for the hexagonal phase of pure SeO₂ crystals can be seen in figure 2 at 2θ = 31.2°, 43.6°, 51.5°, and 56.2° with (101), (102), and (003) reflections. The aforementioned reflections are consistent with the JCPDS standard data (JCPDS Card No. 06-0362) pertaining to this particular phase [9-12]. According to JCPDS 4: 8-0247, the sulfur crystal planes at (113), (222), (313), and (515) are responsible for the peaks at 15.4°, 23.1°, 27.8°, and 47.9° [13-16]. Using the Debye-Scherrer formula [16], it was possible to determine the average crystal size of SeO₂-NPs as 14.69 nm.

AFM is considered to be a highly significant technique for investigating the surface morphology of materials. The

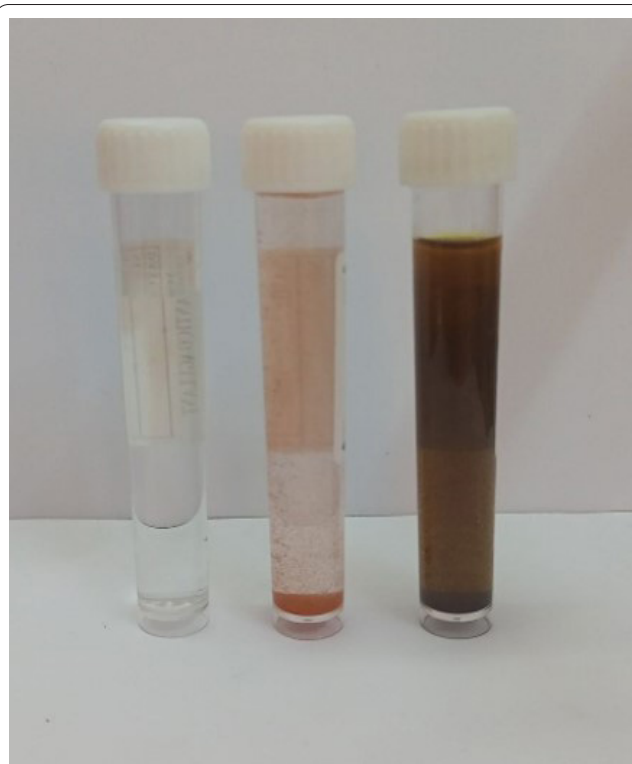


Figure 1: Steps of preparation SeO₂-NPs.

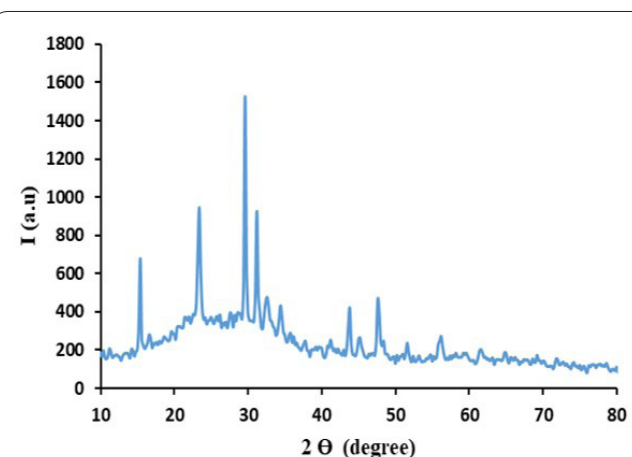


Figure 2: XRD analysis of SeO₂-NPs.

SeO₂-NPs that were produced are depicted in figure 3, showcasing both 2D and 3D AFM images. The 3D image depicts the existence of discrete spherical particles, which is consistent with the findings [17]. The particles exhibit a maximum height of 40.9 nm along the z-axis, an average granular size of 41.07 nm, and a root-mean-square deviation of 8.3 nm. The synthesized SeO₂-NPs exhibit a 2D image that reveals the presence of smaller individual particles measuring approximately 10 nm, as well as larger agglomerates with sizes of up to roughly 100 nm.

The absorbance spectra of SeO₂-NPs, which were synthesized using a chemical method, is illustrated in figure 4. Figure 4 illustrates the distinct absorption peak of SeO₂-NPs. The emergence of a distinct peak at 304 nm is suggestive of the existence of SeO₂-NPs, while a minor peak at 362 nm may indicate the presence of S NPs, as evidenced by the XRD

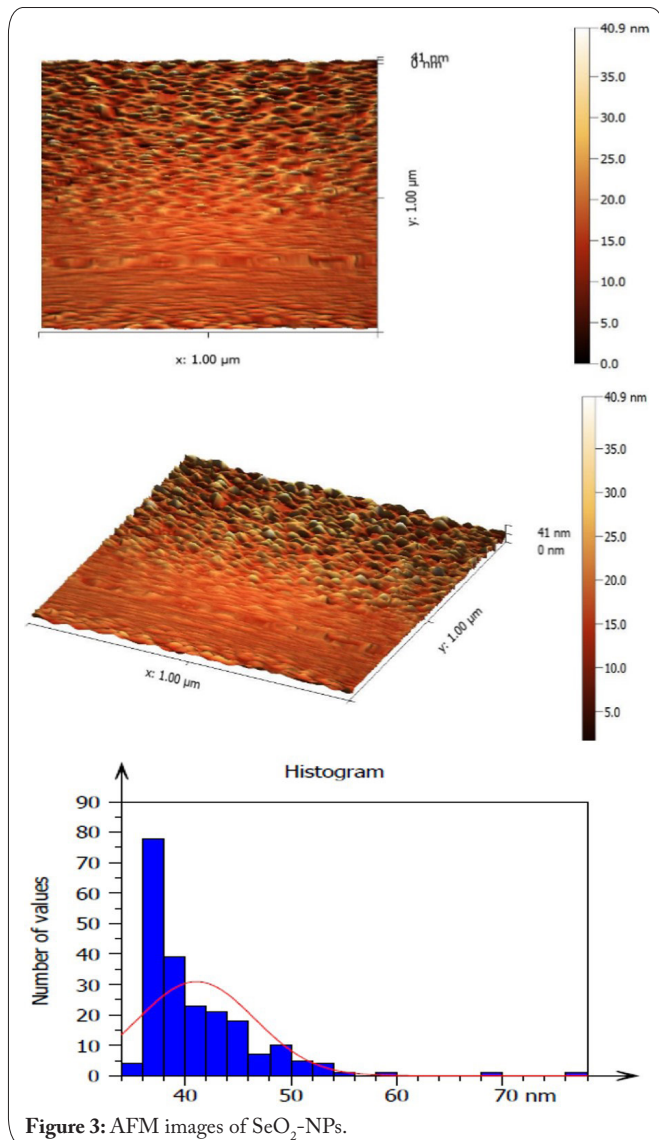


Figure 3: AFM images of SeO₂-NPs.

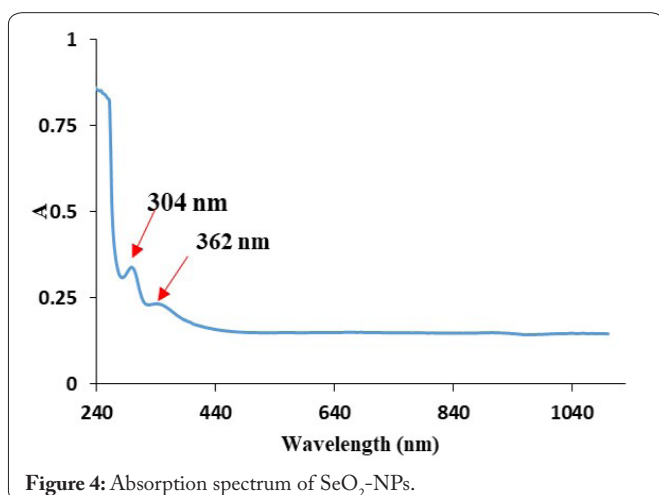


Figure 4: Absorption spectrum of SeO₂-NPs.

findings. The observed phenomenon can be explained by the electronic transition occurring between the valence and conduction band in SeO₂-NPs, which has been previously reported [11, 17]. The value of the optical band gap, as determined from the Tauc' plot (Figure 5), is 3.7 eV. The increase in the band gap value can be attributed to the confinement of the

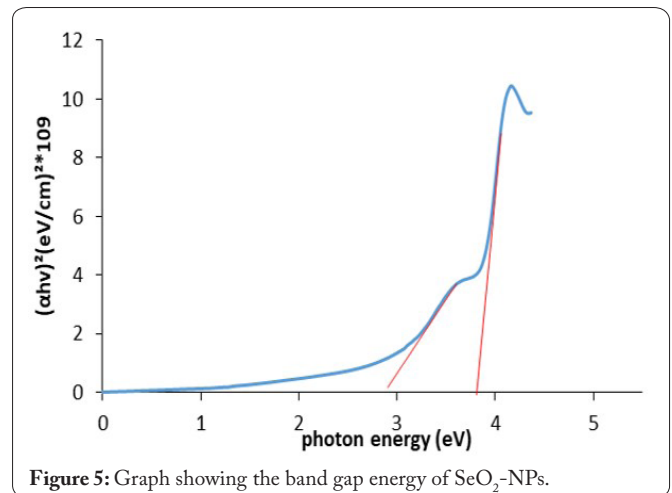


Figure 5: Graph showing the band gap energy of SeO₂-NPs.

size of SeO₂. The confinement effect has a significant impact on the optical characteristics of nanostructure systems, causing a shift towards the blue end of the optical spectra. The shift of the band gap of a semiconductor towards higher energy levels in its bulk form is attributed to the phenomenon of quantum confinement. This transition is attributed to the confinement energy, which is dependent on the substance's dimensions and configuration [18].

FT-IR spectroscopy was employed to ascertain the existence of functional groups within the NPs, as illustrated in figure 6. The peaks observed at 3475 and 1640 cm⁻¹ have been assigned to the O-H and C=C functional groups, respectively. Additionally, the peak observed at 1121 cm⁻¹ has been assigned to the carboxyl group (C=O) present in the SeO₂-NPs, which serve as a stabilizing agent. The vibrational modes of Se=O were found to be associated with the peak observed at 703 cm⁻¹. This observation corroborates the findings of (XRD), which indicated the creation of SeO₂-NPs [19].

Bacteria can be categorized into two distinct classifications, gram-positive and gram-negative bacteria, based on the composition of their cell walls. Gram-positive bacteria are characterized by the presence of a substantial peptidoglycan layer in their cell walls, which confers the ability to retain the crystal violet stain when subjected to the gram staining technique. In contrast to other types of bacteria, gram-negative bacteria are characterized by a relatively narrow cell wall that

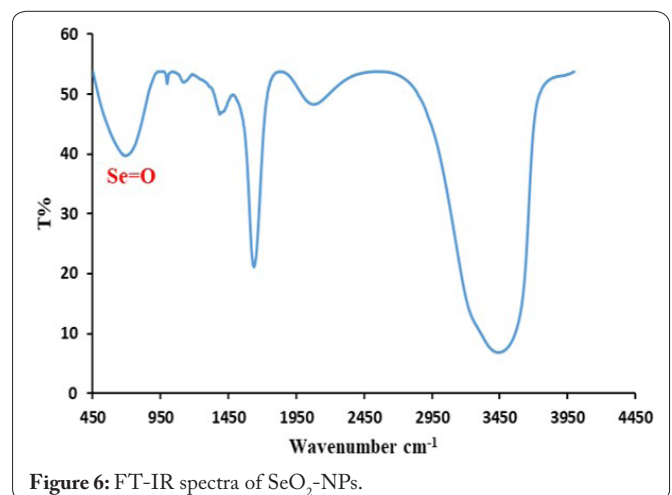


Figure 6: FT-IR spectra of SeO₂-NPs.

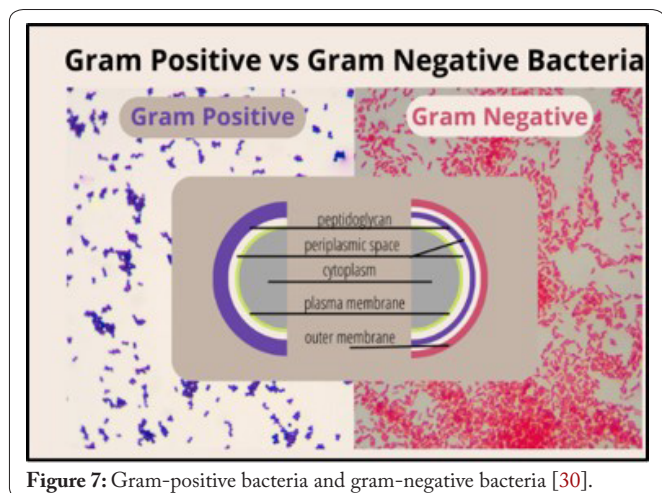


Figure 7: Gram-positive bacteria and gram-negative bacteria [30].

is composed of a layer of peptidoglycan that is encased by an outer membrane. The outer membrane exhibits a lack of retention of the crystal violet stain during the gram staining procedure, as illustrated in figure 7. The cellular wall composition variance significantly affects the pathogenicity of bacteria and the effectiveness of antibiotics. The increased resistance of gram-negative bacteria to antibiotics is frequently attributed to the presence of an outer membrane that acts as a barrier, impeding the penetration of numerous antibiotics, as opposed to gram-positive bacteria [20-24]. The study assessed the antimicrobial efficacy of SeO₂-NPs through the utilization of the agar disc diffusion technique, which involved measuring the zone of inhibition against various bacterial strains and fungi. In summary, the bacterial strains were each inoculated (at a concentration of 10⁵ CFU/ml) onto Mueller-Hinton agar Petri plates using aseptic cotton swabs. Discs with a diameter of 6 mm that had been rendered sterile were immersed in solutions containing SeO₂-NPs at concentrations of 100 µg/ml. The circular objects were meticulously positioned onto sterilized dishes. Following a 24-hour incubation period at 37 °C. The inhibition zone of *S. aureus*, *S. epidermidis*, *Klebsiella*, *E. coli*, and *Candida* is depicted in figure 8. The table 1 displays the diameters of SeO₂-NPs, which have been found to exhibit greater efficacy against gram positive bacteria and fungi. NPs exhibit a cationic charge, thereby enabling their interaction with anionic bacterial and fungal membranes. Upon attachment to the cells, NPs have the ability to traverse the cell membrane or wall, thereby inducing cellular damage. NPs have the potential to interact with bacterial cells through various mechanisms, such as perturbing the cell membrane, inducing oxidative stress, and impeding cellular metabolism. The precise modalities of interaction may exhibit variability contingent upon the NPs variety and bacterial taxonomy [25-30]. The outcomes produced by our method are the best outcomes produced by other researchers when compared to the reference [31].

Table 1: Results of SeO₂-NPs against test bacteria and fungi.

<i>S. aureus</i>	26 mm
<i>S. epidermis</i>	25 mm
<i>E. coli</i>	9 mm
<i>Klebsiella</i>	23 mm
<i>Candida</i>	24 mm

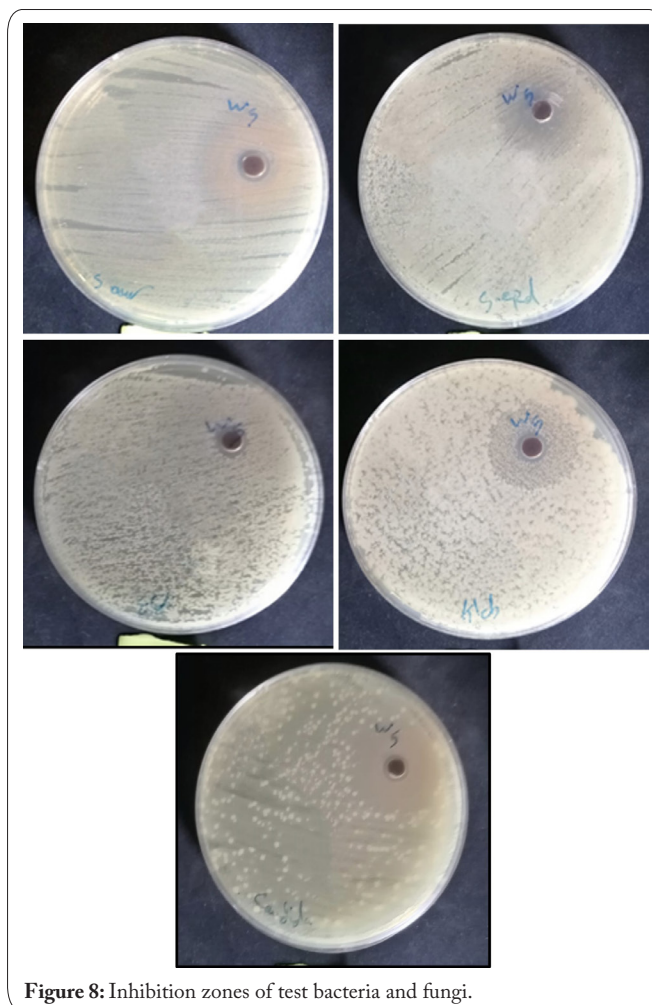


Figure 8: Inhibition zones of test bacteria and fungi.

Conclusion

To conclude, the utilization of SeO₂-NPs with an average grain size of 41.07 nm has exhibited significant potential in the management of bacterial and fungal infections. In addition, the utilization of NPs has the potential to facilitate targeted delivery of antibacterial and antifungal agents to cells, thereby enhancing treatment efficacy and mitigating adverse effects.

Acknowledgements

None.

Conflict of Interest

None.

References

- Hajipour MJ, Fromm KM, Ashkarran AA, de Aberasturi DJ, de Laramendi IR, et al. 2012. Antibacterial properties of nanoparticles. *Trends Biotechnol* 30(10): 499-511. <https://doi.org/10.1016/j.tibtech.2012.06.004>
- Beyth N, Hourri-Haddad Y, Domb A, Khan W, Hazan R. 2015. Alternative antimicrobial approach: nano-antimicrobial materials. *Evid Based Complement Alternat Med* 2015: 246012. <https://doi.org/10.1155/2015/246012>
- Hemeg HA. 2017. Nanomaterials for alternative antibacterial therapy. *Int J Nanomed* 12: 8211-8225. <https://doi.org/10.2147/IJN.S132163>

4. Pelgrift RY, Friedman AJ. 2013. Nanotechnology as a therapeutic tool to combat microbial resistance. *Adv Drug Deliv Rev* 65(13-14): 1803-1815. <https://doi.org/10.1016/j.addr.2013.07.011>
5. Piacenza E, Presentato A, Zonaro E, Lemire JA, Demeter M, et al. 2017. Antimicrobial activity of biogenically produced spherical Se-nanomaterials embedded in organic material against *Pseudomonas aeruginosa* and *Staphylococcus aureus* strains on hydroxyapatite-coated surfaces. *Microb Biotechnol* 10(4): 804-818. <https://doi.org/10.1111/1751-7915.12700>
6. Sadeghian S, Kojouri GA, Mohebbi A. 2012. Nanoparticles of selenium as species with stronger physiological effects in sheep in comparison with sodium selenite. *Biol Trace Elem Res* 146: 302-308. <https://doi.org/10.1007/s12011-011-9266-8>
7. Skalickova S, Milosavljevic V, Cihalova K, Horky P, Richtera L, et al. 2017. Selenium nanoparticles as a nutritional supplement. *Nutrition* 33: 83-90. <https://doi.org/10.1016/j.nut.2016.05.001>
8. Wadhvani SA, Shedbalkar UU, Singh R, Chopade BA. 2016. Biogenic selenium nanoparticles: current status and future prospects. *Appl Microbiol Biotechnol* 100: 2555-2566. <https://doi.org/10.1007/s00253-016-7300-7>
9. Srivastava N, Mukhopadhyay M. 2013. Biosynthesis and structural characterization of selenium nanoparticles mediated by *Zooglea ramigera*. *Powder Technol* 244: 26-29. <https://doi.org/10.1016/j.powtec.2013.03.050>
10. Menon S, Shanmugam V. 2020. Cytotoxicity analysis of biosynthesized selenium nanoparticles towards A549 lung cancer cell line. *J Inorg Organomet Polym Mater* 30(5): 1852-1864. <https://doi.org/10.1007/s10904-019-01409-4>
11. Kazemi M, Akbari A, Zarrinfar H, Soleimanpour S, Sabouri Z, et al. 2020. Evaluation of antifungal and photocatalytic activities of gelatin-stabilized selenium oxide nanoparticles. *J Inorg Organomet Polym Mater* 30: 3036-3044. <https://doi.org/10.1007/s10904-020-01462-4>
12. Abdullah OF, Abulkarem SM, Abad WK. 2022. Selenium dioxide nanoparticles from *Hibiscus sabdariffa* flower extract induce apoptosis in bacterium (gram-negative, gram-positive) and fungi. *NeuroQuantology* 20(3): 198-203.
13. Awwad AM, Salem NM, Abdeen AO. 2015. Novel approach for synthesis sulfur (S-NPs) nanoparticles using *Albizia julibrissin* fruits extract. *Adv Mater Lett* 6(5): 432-435. <https://doi.org/10.5185/am-lett.2015.5792>
14. Chen Z, Sun Z, Zhang Y, Tan T, Tian Y, et al. 2018. Novel sulfur/ethylenediamine-functionalized reduced graphene oxide composite as cathode material for high-performance lithium-sulfur batteries. *Nanomaterials* 8(5): 303. <https://doi.org/10.3390/nano8050303>
15. Suleiman M, Al Ali A, Hussein A, Hammouti B, Hadda TB, et al. 2013. Sulfur nanoparticles: synthesis, characterizations and their applications. *J Mater Environ Sci* 4(6): 1029-1033.
16. Salem FS, Badr MO, Neamat-Allah AN. 2011. Biochemical and pathological studies on the effects of levamisole and chlorambucil on Ehrlich ascites carcinoma-bearing mice. *Vet Ital* 47(1): 89-95.
17. Dwivedi C, Shah CP, Singh K, Kumar M, Bajaj PN. 2011. An organic acid-induced synthesis and characterization of selenium nanoparticles. *J Nanotechnol* 2011: 651971. <https://doi.org/10.1155/2011/651971>
18. Sabouri Z, Akbari A, Hosseini HA, Hashemzadeh A, Darroudi M. 2019. Eco-friendly biosynthesis of nickel oxide nanoparticles mediated by okra plant extract and investigation of their photocatalytic, magnetic, cytotoxicity, and antibacterial properties. *J Clust Sci* 30: 1425-1434. <https://doi.org/10.1007/s10876-019-01584-x>
19. Tripathi K, Husain M, Zulfequar M. 2009. Nano and microstructures of selenium oxide by thermal evaporation. *Chalcogenide Lett* 6(9): 517-522.
20. Sharma G, Sharma AR, Bhavesh R, Park J, Ganbold B, et al. 2014. Biomolecule-mediated synthesis of selenium nanoparticles using dried *Vitis vinifera* (raisin) extract. *Molecules* 19(3): 2761-2770. <https://doi.org/10.3390/molecules19032761>
21. Jassim AM, Farhan SA, Salman JA, Khalaf KJ, Al Marjani MF, et al. 2015. Study the antibacterial effect of bismuth oxide and tellurium nanoparticles. *Int J Chem Biomol Sci* 1(3): 81-84.
22. Apsana G, George PP, Devanna N, Yuvasravana R. 2018. Biomimetic synthesis and anti-bacterial properties of strontium oxide nanoparticles using *Ocimum sanctum* leaf extract. *Asian J Pharm Clin Res* 11(3): 384-389. <https://doi.org/10.22159/ajpcr.2018.v11i3.20858>
23. Roy A, Bulut O, Some S, Mandal AK, Yilmaz MD. 2019. Green synthesis of silver nanoparticles: biomolecule-nanoparticle organizations targeting antimicrobial activity. *RSC Adv* 9(5): 2673-2702. <https://doi.org/10.1039/c8ra08982e>
24. Wakshlak RBK, Pedahzur R, Avnir D. 2015. Antibacterial activity of silver-killed bacteria: the "zombies" effect. *Sci Rep* 5(1): 9555. <https://doi.org/10.1038/srep09555>
25. Vazquez-Muñoz R, Meza-Villezas A, Fournier PGJ, Soria-Castro E, Juarez-Moreno K, et al. 2019. Enhancement of antibiotics antimicrobial activity due to the silver nanoparticles impact on the cell membrane. *PLoS One* 14(11): e0224904. <https://doi.org/10.1371/journal.pone.0224904>
26. Li WR, Xie XB, Shi QS, Zeng HY, Ou-Yang YS, et al. 2010. Antibacterial activity and mechanism of silver nanoparticles on *Escherichia coli*. *Appl Microbiol Biotechnol* 85: 1115-1122. <https://doi.org/10.1007/s00253-009-2159-5>
27. Jabbar MA, Abad WK, Abd AN. 2023. Green syntheses of CdO NOs: the biological efficacy study against human pathogens (*E. Coli* and *Candida*). *HIV Nursing* 23(3): 1662-1666.
28. Hu S, Yi T, Huang Z, Liu B, Wang J, et al. 2019. Etching silver nanoparticles using DNA. *Mater Horiz* 6(1): 155-159. <https://doi.org/10.1039/c8mh01126e>
29. Sadoon AA, Khadka P, Freeland J, Gundampati RK, Manso RH, et al. 2020. Silver ions caused faster diffusive dynamics of histone-like nucleoid-structuring proteins in live bacteria. *Appl Environ Microbiol* 86(6): e02479-19. <https://doi.org/10.1128/AEM.02479-19>
30. Qing YA, Cheng L, Li R, Liu G, Zhang Y, et al. 2018. Potential antibacterial mechanism of silver nanoparticles and the optimization of orthopedic implants by advanced modification technologies. *Int J Nanomed* 13: 3311-3327. <https://doi.org/10.2147/IJN.S165125>
31. Baqi ZH, Nasser ZS, Sulaiman LH, Abd AN. 2022. The anti-bacterial activity of selenium dioxide nano-particles and prospects for the future. *J Phys Conf Ser* 2322(1): 012085. <https://doi.org/10.1088/1742-6596/2322/1/012085>